Large and Fast Relaxations inside a Protein: Calculation and Measurement of Reorganization Energies in Alcohol Dehydrogenase

Ross C. Walker,[†] Melanie M. de Souza,[‡] Ian P. Mercer,[‡] Ian R. Gould,[†] and David R. Klug*,[‡]

Biophysics and Biological Chemistry Group and Molecular Dynamics Group, Department of Chemistry, Imperial College of Science, Technology and Medicine, London, U.K.

Received: May 24, 2002; In Final Form: August 30, 2002

We have used a recently established quantum mechanics/molecular mechanics (QM/MM) method[1] to calculate the optical absorption and emission spectra for NADH in liver alcohol dehydrogenase. The widths of these spectra are sensitive to the amplitude and time scale of protein fluctuations, while the Stokes shift is a direct measure of the extent of relaxation of the molecular system. Despite the very large Stokes shift in this system (∼0.9 eV), we find that the reorganization energy is recovered with 13% accuracy. Moreover, the spectral widths are within 6% of the experimental values. Our results demonstrate that our QM/MM approach to the calculation of free energy surfaces remains highly viable even for very large and very fast fluctuations and even for systems as complex as proteins. We also show that the quality of the results very much depend on the quality of the molecular dynamics trajectory and as such our method provides a way to validate molecular mechanics force field parameters for chromophores via direct comparison with experiment.

Introduction

The extent of a chemical reaction is determined by the free energy difference between reactants and products. The rate constant for a catalytic step is greatly affected by the free energy of activation. It would be useful therefore to be able to predict the extent, origin, and rate of development of this free energy difference in condensed-phase chemical reactions. A liquid or protein will respond to a rapid change in charge distribution by structural rearrangements that minimize the energy of the system. The energy associated with these rearrangements is generally termed the reorganization energy and has a well-established role in, for example, nonadiabatic electron-transfer theory. The reorganization energy also appears in the response of a condensed-phase chemical system to optical excitation. The creation of an excited electronic state rearranges the electron density in the molecule, leading to a rearrangement of the surrounding medium and a lowering of the excited-state energy and concomitant raising of the ground-state energy. In fluorescent systems, reorganization is revealed by the fluorescence Stokes shift, which is proportional to the reorganization energy of the system.

In one sense, creation of an excited state and the subsequent Stokes shift of the fluorescence can be regarded as an extremely simple type of chemical reaction. The reactant in this case is the excited state of the molecule initially created by the applied optical field, and the product is the state created by relaxation of the system. The free energy gap between reactants and products is indicated by the shift in the peak of the steady-state absorption band from that of the steady-state emission band. The steady-state emission spectrum is a good representation of the product energy because most of the relaxation is complete well before the excited-state emits a photon. Moreover, the spectral width of the absorption and emission spectra reflect

the time scale of the fluctuations, as is apparent from optical response theory (see Appendix B).

Attempts to calculate the free energy difference between initial and relaxed states in optically excited systems are a natural first step prior to calculating free energy gaps, free energies of activation, and relaxation rates during more complex chemical processes.

Classical molecular dynamics in conjunction with classical evaluation of energy gaps has previously been applied to the calculation of optical properties of smaller solvated molecules. This yielded predictions of the shifts of the absorption and emission maxima between vacuum and solvent of indole and 3MI,[2] the Stokes shift of coumarin 153,[3] and the Stokes shift and dynamics fluorescence shift of coumarin 343.[4,5]

We have previously used a quantum mechanical/molecular mechanical (QM/MM) method to calculate the relaxations in solvated chlorophylls[1,6] and zinc and iron myoglobin[7,8] and found that it reproduced both the reorganization energies and the spectral widths to within 20% of their experimental values. In this paper, we use the same method to calculate much larger relaxations in the enzyme alcohol dehydrogenase.

The Stokes shift in dihydronicotinamide adenine dinucleotide, NADH, the chemically active cofactor in alcohol dehydrogenase and many other enzymes, is 1.04 eV (100.36 kJ/mol) in water. This is reduced to 0.87 eV when bound to the protein matrix of horse liver alcohol dehydrogenase (LADH, in the context of this paper always complexed with NADH) with the inhibitor *n*-cyclohexyl formamide in the substrate binding site. In this work, we have performed classical molecular dynamics calculations for LADH inhibited with *n*-cyclohexyl formamide using the AMBER 6.0 suite of molecular dynamics programs.[9] We subsequently used these trajectories to calculate fluctuating ground- to excited-state energy gaps for the NADH cofactor as a function of time. From this, we have calculated optical absorption and emission spectra and hence Stokes shift of LADH for three different molecular dynamics force field parameters. This allows the sensitivity of the spectra to the force field to be

* To whom correspondence and reprint requests should be addressed.
[†] Biophysics and Biological Chemistry Group.
[‡] Molecular Dynamics Group.

Large and Fast Relaxations inside a Protein

J. Phys. Chem. B, Vol. 106, No. 44, 2002 **11659**

tested, as well as determination of the accuracy of our methodology. The large relaxation of LADH provides a severe test of our approach as the assumption of linear response is pushed to the limit by such a large deviation from equilibrium. Despite this, we find that the experimental Stokes shift/reorganization energy is determined to better than 13% accuracy.

LADH[10] is a very well characterized enzyme which, with the use of NAD$^+$ as a cofactor, catalyses the reversible oxidation of a wide range of alcohols to their corresponding aldehydes. It has a molecular weight of 80 000 and is composed of a dimer of two identical parts as reported in the X-ray structure.[11] Each subunit of the dimer binds one molecule of NADH and two Zn(II) ions. One zinc is in the active site and is associated with the aldehyde oxygen of the substrate or substrate analogue, while the other zinc performs a structural role. At pH 7, the equilibrium position of the chemistry favors NAD$^+$ and alcohol,[12] and we therefore use the LADH−NADH−*n*-cyclohexyl formamide ternary complex as the system of study.

Methodology

Amber Force Field Parametrization. The initial starting structure for LADH included *n*-cyclohexyl formamide as an inhibitor and was obtained from the crystal structure of horse liver LADH by Ramaswamy et al.[11] (RCSB Protein Data Bank 1LDY). The asymmetric unit contains two dimers in close proximity. The first of the two dimers (chains A and D in the pdb) was used as the initial configuration. The extracted coordinates were prepared for the molecular dynamics simulations using the xLEaP module,[13] which forms part of the AMBER 6.0 suite of molecular dynamics programs.[9] On the basis of an examination of the hydrogen bonds by Ryde,[14] histidine residues 34, 67, 138, and 139 were defined as being protonated on the δ nitrogen (HID), histidine residue 105 on the ϵ nitrogen (HIE), and histidine residues 51 and 348 on both nitrogens (HIP) and thus positively charged. All of the six cysteine zinc ligands, Cys46, Cys97, Cys100, Cys103, Cys111, and Cys174, were assumed to be negatively charged[14,15] (CYM), while the remaining eight cysteine ligands were assumed to be neutral (CYS). Because the structural zinc is a large distance from the NADH active site (∼16 Å), it was defined as a hard sphere ion of charge 2+ and was not explicitly bonded to any of the four surrounding cysteine residues. The catalytic zinc atom, however, is close to the NADH active site and so was parametrized explicitly.

Four-coordinate zinc is believed to be more stable than five-coordinate,[14,16] so the catalytic zinc atom was bonded to the two nearby cysteine residues (residues 46 and 174), the oxygen atom of the *n*-cyclohexyl formamide inhibitor (residue 378), and the ϵ nitrogen of the nearby histidine (residue 67).

Force field parameters not defined in the standard Amber force field[17] were obtained from existing published parameters or by analogy with the standard residues. For the catalytic zinc, these were taken from published computational studies of the catalytic zinc ion by Ryde,[14] while those for *n*-cyclohexyl formamide were derived from comparison with the parameters for standard amino acid residues.

Three different parameter sets were used for the NADH residue. The NADH was defined as a nonstandard residue, and in all three cases, the adenine dinucleotide, diphosphate and the two ribose sections were parametrized from analogy with the standard amino acid residue library in AMBER 6.0. The adenine moiety of NADH was taken from the adenine residue defined in the Amber force field. The two ribose and attached phosphate groups were copied from the default template for a DNA backbone, while the nicotinamide section was parametrized in a different way for each of the three classical MD simulations conducted.

In the first simulation, the parameters used for the nicotinamide section of NADH were those published by Pavelites et al.[18] In the second and third sets of simulations, parametrization was based on simple analogy using the atom types and parameters defined in Appendix A. Equilibrium angles that were missing from the default Amber force field were found by conducting ab initio geometry optimizations on dihydronicotinamide truncated with a methyl group on the ring nitrogen using Hartree−Fock theory[19] with the SV 3-21G*[20] basis set implemented in the program Gaussian 98.[21] The missing stretching, bending, and torsional terms were adapted from existing parameters. The reason for doing this was to investigate how sensitive our method was to the quality of the molecular dynamics parameters. The method detailed above resulted in a force field that, while reasonably good, was not strictly parametrized in the thorough method employed by Pavelites et al.[18] The variation between the second and third simulations concerned the parametrization of the amide moiety of the NADH cofactor (atoms N7, O14, C18, H67, and H73, Appendix A, Table 4). Trial calculations showed that the molecular orbitals involved in the excitation corresponding to NADH absorption and emission are highly dependent on the structure of this amide group. Hence it was believed that the accurate parametrization of this moiety would be essential to obtaining good results. Thus for the second simulation, we used our simple analogy-based force field but kept the torsions defined by Pavelites et al.[18] for the amide moiety. Because the magnitude of these torsions are very small in comparison to, for example, a peptide linkage, we decided to, for the third simulation, simply set these torsions to zero. The results from all three simulations are presented here.

The hydrogen atoms, not present in the crystal structure, were added at idealized bond lengths and angles as necessary to fulfill valence requirements. The LADH dimer was then neutralized by the addition of four Cl$^-$ ions distributed in a shell around the LADH dimer using a Coulombic potential on a 1 Å grid. The whole system was then solvated using the TIP3P[22] water model by placing it in a box of dimensions 83.51 × 128.12 × 86.55 Å^3 containing approximately 21 000 water molecules to yield a system of 76 723 atoms with an average density of 0.849 g cm^{-3}.

Atom-centered point charges for the nonstandard residues were derived for the ground state using density matrices obtained from Hartree−Fock[19] SV 6-31G*[20] calculations in accordance with the RESP[23] method for the Amber force field.[17] Appendix A gives details of the nonstandard parameters and atom-centered charges used in the various simulations.

Molecular Dynamics Protocol. Three separate but procedurally identical molecular dynamics (MD) simulations were performed on the dimer system in a bath of water molecules for the three force field configurations detailed above. The protocol used for the MD simulations was as follows. The system was first subjected to 200 steps of steepest descent followed by 300 steps of conjugate-gradient minimization on just the solvent molecules followed by 200 steps of steepest descent and 800 steps of conjugate-gradient minimization on the whole system to alleviate incorrect van der Waals contacts created by hydrogenation and solvation of the system. A residue-based nonbonded cutoff of 12 Å was used for this and all subsequent simulations. The system was then subjected to 20 ps of slow heating from 0 to 300 K using independent scaling of the velocities of the solute and solvent following the method

of Berendsen[24] to control the temperature. In all MD simulations, constant pressure periodic boundary conditions using the particle mesh Ewald method[25] were employed, the integration time step was set at 1 fs, and all interactions were calculated at every step. No atoms had their positions fixed or their motions damped.

After slow heating, the system was equilibrated for 100 ps at 300 K. Equilibration was deemed to have been successfully obtained when the root-mean-square deviation (rmsd) of the protein α carbons was reasonably small (<0.9 Å) and both the rmsd and classical energies of the system fluctuated by less than 10% over a time scale of approximately 20 ps. An energy gap production run was then performed for the subsequent 10 ps with the complete system coordinates being recorded every 2 fs, resulting in a trajectory of 5000 coordinate sets. This entire process was then repeated for each of the three parameter sets.

Quantum Mechanical Calculation of Energy Gaps. The theory used for calculating optical spectra from a fluctuating energy gap has been discussed in a previous paper[1] but for the benefit of the reader has been reproduced in full in Appendix B. This method requires calculation of an energy gap correlation function with an energy gap calculated every 2 fs for 5 ps.

The trajectories obtained from the 10 ps production runs of the MD simulations were used to create time-ordered structures for the QM calculations. The QM method employed in this study is implemented within the ab initio package Gaussian 98.[21] The method consists of incorporating the point charges of the water and protein surrounding the selected NADH residue into the one-electron Hamiltonian. This has the effect of polarizing the wave function with respect to the protein structure and solvent distribution.

Taking structures from the classical MD trajectories, single-point configuration interaction singles (CIS)[26] calculations utilizing the 3-21G*[20] basis set were performed to calculate the singlet energy gap between the ground and first excited state for the system of interest at 2 fs intervals. The use of the 3-21G* basis set was to ensure that the calculations were tractable to the available computing resources. Trial CIS calculations showed that the orbitals involved in the excitation were centered purely on the nicotinamide moiety of the NADH, and thus it was decided to treat the chosen NADH residue quantum mechanically, while treating the rest of the protein and surrounding waters classically, giving a system consisting of 71 atoms corresponding to 470 basis functions. In this way, the need for link atoms was negated because the NADH residue is not formally bound to the protein matrix. The point charges of the classical system were included in the one-electron Hamiltonian of the quantum element of the calculations.

For all three simulations, a total of 2500 points representing the first 5 ps of the 10 ps production runs were calculated for both NADH residues (ID numbers 375 and 753) yielding a total of 5000 CIS calculations per dimer. Calculating the energy gaps independently for each NADH residue led to two different absorption and emission spectra being produced, one for each NADH residue. The spectra shown are produced by averaging the spectra from the two NADH binding sites of the LADH dimer. The calculated absorption and emission spectra are shifted in energy by the same amount such that the peaks of the calculated absorption spectrum coincide with those of the experimental spectrum. By these means, each method's ability to predict the extent of relaxation becomes apparent by comparing the experimental and calculated Stokes shifts. This emphasizes the aim of our work, which is to calculate relaxation energies rather than equilibrium energies. For the record, the

CIS method together with the 3-21G* basis set gives an average transition energy of approximately 5.1 eV.

The absorption and emission spectra were generated from the time-correlated energy gap fluctuations by utilizing the methodology of Mercer et al.[1,6] Our previous calculations and arguments based on the nature of electron vibration coupling in proteins had shown that we could expect a reasonable convergence of the Stokes shift within 5 ps. We chose our convergence criteria as previously with this methodology, namely, that convergence was deemed to have occurred once the change in predicted Stokes shift was less than 10% for a doubling of the run length.

Experimental Measurement of Spectra. LADH (0.52 units/ mg solid, 0.87 units/mg protein) and NADH (98% pure) were obtained from Sigma-Aldrich and used without further purification. *n*-Cyclohexyl formamide (CXF) (Sigma-Aldrich) was purified using a silica gel column developed with ethyl acetate and hexane (60/40). All solutions were made up in phosphate buffer (pH 7.4) and were checked for extraneous fluorescence. To ensure that all of the NADH was in the bound state, an excess of LADH was used in the ternary complex. The absorption and emission spectra of the ternary complex (ratio 3:1:100 of LADH/ NADH/CXF in phosphate buffer solution, pH 7.4) are shown with calculated spectra in Figures 1, 2, and 3. To validate that sufficient CXF was present, a number of emission spectra were measured for varying ratios of CXF to protein from 35% to 93.4%. It was found that over this range the difference in Stokes shift was 0.034 eV implying that the emission peak position was largely unaffected by the CXF to protein ratio.

The electronic absorption spectra were recorded on a UV− vis spectrophotometer (Shimadzu) and the luminescence spectra on a photon-counting spectrometer (SPEX Fluoromax).

The complete absorption spectra of the nicotinamide moiety of NADH bound to LADH cannot be obtained because of the extremely intense absorption of the NADH adenine group in the range 3.9 to 5.1 eV. Thus it was necessary to reconstruct the absorption spectra due to the nicotinamide moiety beyond the 3.95 eV range by taking the profile of the absorption spectra for unbound NADH in water, which is better resolved from the adenine absorption, and overlaying this on the NADH + LADH ternary complex absorption spectra. This method was justified because it was found that both spectra are close to Gaussian and have widths within 5% of each other.

Results

The major results are summarized by the optical absorption and emission spectra for each of the three simulations shown in Figures 1, 2, and 3 corresponding to the first, second, and third MD simulations, respectively.

Figure 1 shows the results obtained for the first MD simulation in which the published NADH parameters of Pavelites et al.[18] were employed. These show reasonably good agreement with the experimental spectra considering that the assumption of linear response is being used. The Stokes shift is reported as 0.984 eV, which compared with the experimental value of 0.872 eV agrees to 13%. The widths are reproduced to within 6% of experiment.

Figure 2 shows the results obtained from the second MD simulation in which only the NADH amide moiety torsions were based on those of Pavelites et al.[18] The remaining NADH parameters were defined on a simple analogy-based approach. It can be seen from Figure 2 that the calculations agree much less well with experiment, yielding a Stokes shift prediction of only 0.481 eV compared with an experimental value of 0.872

Large and Fast Relaxations inside a Protein

J. Phys. Chem. B, Vol. 106, No. 44, 2002 **11661**
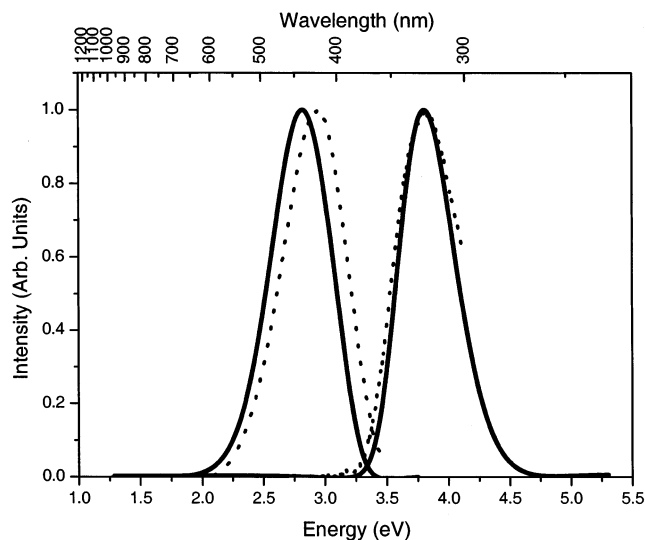
Figure 1. Optical absorption and emission spectra for LADH + NADH in water showing comparison between theory (solid) and experiment (dotted) for the NADH parameters published by Pavelites et al., the most accurate set of parameters used in this study.
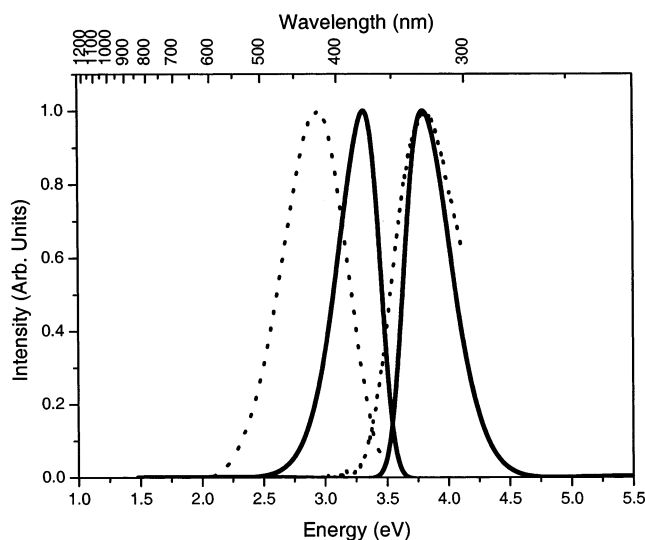
Figure 2. Optical absorption and emission spectra for LADH + NADH in water showing comparison between theory (solid) and experiment (dotted) for the second simulation in which only the NADH amide moiety torsions were based on those published by Pavelites et al. while the remaining NADH parameters were defined from a simple analogy-based parametrization. The agreement between calculation and experiment is clearly worse than with the properly parametrized force field.

eV, an error of 55%. The absorption and emission spectral widths are also considerably worse, showing a 39% deviation from experiment. This shows that our method is very sensitive to the force field parameters used. The reduced Stokes shift in this case suggests that the dynamics of the system have not been adequately explored by the molecular dynamics trajectory.

In Figure 3, we see that when a force field with zero torsions for the NADH amide moiety is used the results obtained are very poor with two distinct peaks due to the two NADH residues having distinctly different behaviors in the binding sites.

Discussion

The key result of these calculations is that using a properly parametrized force field for the molecular dynamics we recovered the Stokes shift/reorganization energy to an accuracy
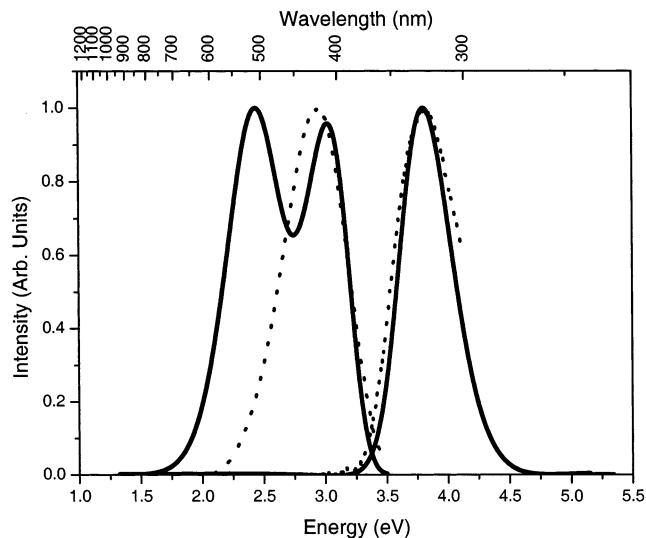
Figure 3. Optical absorption and emission spectra for LADH + NADH in water showing comparison between theory (solid) and experiment (dotted) for the third simulation in which the analogy-based approach to parametrization was used but with the torsions for the amide moiety of the NADH set to zero.

better than 13%. We have previously shown a similar level of accuracy for reorganization energies in the case of solvated chlorophyll and bacteriochlorophyll[1,6] and more recently in iron and zinc myoglobin.[7,8] It is rather encouraging to find that the methodology works this well for the large relaxations in alcohol dehydrogenase. It is at first sight somewhat surprising that the assumption of linear response holds so well for a system that shows a Stokes shift of almost 0.9 eV out of an energy gap of approximately 4 eV. The success of our approach requires the spectrum of coupled oscillators, which provide the electron-vibration coupling, to be essentially the same in the ground and excited states of NADH. We know of only one other case in which linear response theory has been tested on a system with a very large reorganization energy, the work of Chandler et al. who successfully showed that the assumption of linear response did not prevent the accurate recovery of free energies of activation for an Fe^{2+}/Fe^{3+} redox couple.[27] It is at first sight somewhat surprising that there is no need to keep recalculating the partial charges as the molecular dynamics calculation progresses; however, we have now shown that this QM/MM approach succeeds in reproducing reorganization energies to within 20% accuracy in five different chemical systems,[1,6-8] including three proteins. By using only one set of ground-state partial charges to drive the MD, we are rigorously applying the linear response constraint, and the reasonable accuracy that this confers strongly suggests that the electron-vibration coupling (spectrum of oscillators) remains essentially unchanged from the initial absorption of a photon until the relaxation of the system is complete. It may be that the residual inaccuracy of 10−20% reflects the limitations of the linear response approach. Overall however, these results provide some hope that this methodology may be successfully applied to determine the free energy of activation in reactive systems.

The sensitivity of the reorganization energy to the parameter set chosen for the NADH chromophore suggests that the large Stokes shift observed in LADH comes largely from internal vibrations of the nicotinamide moiety and not from the protein matrix or from solute−solvent interactions. This is further supported by the observation that the absorption and emission profiles of NADH bound to LADH and NADH in water are essentially identical. The only spectral differences are in the

form of a blue shift in the spectra when bound to the LADH protein matrix. The Stokes shift/reorganization energy is 16.3% smaller in the LADH + NADH case compared with NADH in water. This again suggests that it is the degrees of freedom internal to the NADH that dominate the reorganization energy.

The sensitivity to MD parameters is also worthy of comment. It is not immediately obvious that the overall electron-vibration coupling calculated by our QM/MM approach would be very sensitive to the details of the molecular dynamics force field. We find, however, that the method is actually rather sensitive to the MD parameters. A comparison of three parameter sets broadly demonstrates this point and is not intended to be an exhaustive assessment of the dominant contributions to the electron-vibration coupling. To achieve such an analysis would require a normal-mode analysis of the spectrum of oscillators and is outside the scope of this publication. The parameter set of Pavelites et al. has reasonably low values for the NADH-amide dihedral parameters (0.5−2.5 kcal/mol). One might imagine that a freely rotating amide might simulate this rather well; however, Figure 3 demonstrates that this is not the case. Moreover, when we switched off the NADH-amide torsion parameters, we found that the root-mean-square deviation (rmsd) for the NADH residue actually decreased from 0.763 to 0.498 Å. A lower rmsd is usually associated with a better representation of the system. However, we find that for LADH + NADH this is not the case. The counter example of this is to use very stiff torsional terms. When we examined this variation (using dihedral parameters of ∼12 kcal/mol), we found that the Stokes shift became far too small (<0.3 eV). These results demonstrate that our QM/MM methodology is a sensitive, if expensive, validator for molecular dynamics trajectories of fluorescent chromophores via direct comparison with experiment.

Conclusions

We have demonstrated that a previously used QM/MM method is capable of accurately predicting large reorganization energies in a protein. In the case of LADH, the calculated reorganization energy is found to be within 13% of the experimental value. We have also shown that our method is sufficiently sensitive to the parameters used for the molecular dynamics simulation that it provides a method for validating molecular dynamics parameters for fluorescent chromophores.

Appendix A. Nonstandard Parameters and Charges Used for the Various MD Simulations

Tables 1−4 give details of the nonstandard parameters and atom-centered charges used in the various simulations. The nomenclature used for atom types and parameters is the same as that used in the Cornell et al. force field.[17] When parameters are not explicitly defined, they are available as part of the standard Cornell et al. force field[17] or are available in the referenced papers of Ryde[14−16] and Pavelites et al.[18]

Appendix B. Obtaining Absorption and Emission Spectra from a QM/MM Simulation[1,6]

The incident light field is taken to interact with two electronic levels, the ground and lowest excited singlet state of the molecule. The energy of these levels fluctuates as a result of interactions with the surrounding bath, resulting in a time-

TABLE 1: Nonstandard MD Parameters and Charges for the *n*-Cyclohexyl Formamide Inhibitor
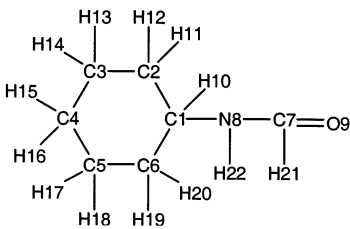
CXF Atom Types and Charges

atom	type	charge	atom	type	charge
C1	CT	−0.047 093	H12	HC	+0.014 835
C2	CT	−0.013 558	H13	HC	+0.003 181
C3	CT	+0.005 532	H14	HC	+0.003 181
C4	CT	+0.018 703	H15	HC	+0.001 954
C5	CT	−0.021 191	H16	HC	+0.001 954
C6	CT	−0.038 157	H17	HC	+0.016 289
N8	N	−0.251 314	H18	HC	+0.016 289
C7	C	+0.298 933	H19	HC	+0.029 578
O9	O	−0.387 555	H20	HC	+0.029 578
H10	H1	+0.143 500	H21	H2	+0.069 656
H11	HC	+0.014 835	H22	H	+0.240 420

Missing CXF Bond Parameters

bond type	K_r (kcal/mol)	r_{eq} (Å)
C−H2	367.0	1.080

Missing CXF Angle Parameters

angle type	K_θ (kcal/mol)	θ_{eq}
N−C−H2	35.0	113.2
O−C−H2	35.0	122.3

varying Bohr frequency. The time evolution of this system is described by the Liouville−von Neumann equation,[28]

$$\frac{d\rho(t)}{dt} = -\frac{i}{\hbar}[(H(t),\rho(t))] \quad (1)$$

where $\rho(t)$ is the density operator for a two-level system with levels a and b and $H(t)$ is the Hamiltonian operator. Following an optical interaction at $t = 0$ and assuming no population loss, the solution to eq 1 is given by

$$\rho_{ab}(t) = \rho_{ab}(0)\exp(-i\omega_{ab}t)\langle\exp\{-i\int_0^t \delta\omega_{ab}(\tau)\,d\tau\}\rangle \quad (2)$$

The angled brackets represent averaging over an ensemble of molecules, $\rho_{ab}(t)$ is an off-diagonal element of the density matrix, ω_{ab} is the mean angular frequency associated with the electronic energy gap, $\delta\omega_{ab}$ is the fluctuation of the energy gap from the mean value, and t is the time of the second interaction with the light field.

Finding the polarization of the ensemble requires taking the trace of the product of the transition dipole operator with the density matrix. Within the rotating wave approximation, this yields the linear optical response function, $R(t)$,

$$R(t) = \langle\mu(t)\mu(0)\exp(i\int_0^t \delta\omega_{ab}(\tau)\,d\tau)\rangle \quad (3)$$

where $\mu(t)$ and $\mu(0)$ are the transition dipole operators at times t and 0, respectively.

Taking the distribution of fluctuations of the energy gap to be Gaussian and assuming that sufficient phase space has been sampled, the cumulant expansion[29] can be applied to eq 3. Taking the transition dipole moment (TDM) to be constant in

Large and Fast Relaxations inside a Protein

J. Phys. Chem. B, Vol. 106, No. 44, 2002 **11663**

TABLE 2: Nonstandard MD Parameters and Charges for the Catalytic Zinc Bound Cysteines[a]
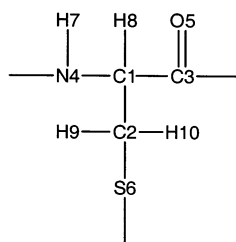
Catalytic Zinc Bound Cysteines Atom Types and Charges

atom	type	charge CYA	charge CYB	atom	type	charge CYA	charge CYB
C1	CT	+0.019 95	−0.007 67	S6	SH	−0.542 71	−0.569 20
C2	CT	−0.096 17	−0.201 92	H7	H	+0.252 98	+0.298 37
C3	C	+0.639 48	+0.608 35	H8	H1	+0.132 91	+0.118 11
N4	N	−0.489 26	−0.464 42	H9	H1	+0.093 45	+0.127 08
O5	O	−0.592 08	−0.571 08	H10	H1	+0.093 45	+0.127 08

[a] CYA = residue 46; CYB = residue 174.

TABLE 3: Nonstandard MD Parameters and Charges for the Catalytic Zinc Bound Hystidine

Catalytic Zinc Bound Histidine Atom Types and Charges

atom	type	charge	atom	type	charge
C1	CT	−0.096 079	O10	O	−0.498 915
C2	CT	−0.088 318	H11	H1	+0.135 500
C3	C	+0.529 423	H12	H	+0.209 094
C4	CC	−0.034 573	H13	HC	+0.092 702
C5	CV	−0.029 486	H14	HC	+0.092 702
C6	CR	−0.034 573	H15	H4	+0.188 232
N7	N	−0.335 847	H16	H	+0.272 147
N8	NA	−0.038 078	H17	H5	+0.161 570
N9	NB	−0.242 772			

time (Condon approximation) and setting it to unity, the response function then becomes

$$R(t) = \exp(-g(t)) \tag{4}$$

where $g(t)$, the line broadening function, is given by

$$g(t) = \Delta^2 \int_0^t d\tau_1 \int_0^{\tau_1} M(\tau_2) \, d\tau_2 \tag{5}$$

and $M(t)$ is the autocorrelation function of the energy gap fluctuations scaled to unity,

$$M(t) = \frac{1}{\Delta^2} \int_{-\infty}^{\infty} \delta\omega_{ab}(t+\tau)\delta\omega_{ab}(\tau) \, d\tau \tag{6}$$

where Δ is the root-mean-square deviation of the energy gap fluctuations.

Note that the ensemble average of eq 3 is now reproduced using the autocorrelation of a single variable, namely, the deviation from the frequency associated with the mean energy

gap, $\delta\omega_{ab}$. It is this frequency deviation that is delivered by the QM/MM simulations.

The steady-state absorption and emission spectra are Fourier-related to the linear response function in time (eqs 3 and 4) and are given by the following:[28,30]

$$\sigma_{abs}(\omega) \propto \text{Re}[\int_0^t dt \, R(t) \exp[i(\omega - \omega_{ab})t]] \tag{7a}$$

$$\sigma_{emis}(\omega) \propto \text{Re}[\int_0^t dt \, R(t) \exp[i(\omega - \omega_{ab})t]] \tag{7b}$$

To find the emission spectrum, it is assumed that the excited-state potential energy surface has the same profile as that of the ground state but with a minimum shifted along the relaxation coordinate. This assumption is made for convenience to save computational cost. The fact that the profiles for the experimental absorption and emission spectra are not quite identical demonstrates that the assumption is approximate.

Up to this point, the response function, $R(t)$, has been taken to be real, and as such, eqs 7a and 7b are identical; there is no spectral shift between the emission and absorption spectra. To introduce a Stokes shift, $M(t)$ is modified to satisfy detailed balance, imparting a complex component. By asserting detailed balance, we make the response of the system conform to the fluctuation−dissipation theorem.[31] In the context of this work, the fluctuation−dissipation theorem connects the fluctuations of an electronic energy level to its rate of relaxation following displacement from equilibrium.

Detailed balance is included by operating on the spectrum of oscillators, $J(\omega)$, which is given by the Fourier transform of $M(t)$. Because $M(t)$ is real and symmetric, $J(\omega)$ is necessarily also real and symmetric. However, to satisfy detailed balance, it is required that positive frequencies should be related to their negative counterparts by a Boltzmann coefficient[32] such that

$$J(-\omega) = \exp(-\hbar\omega/(kT))J(\omega) \tag{8}$$

To satisfy this relationship, a modified semiclassical form of the spectral density is given by[33]

$$J_{SC}(\omega) = \frac{2J(\omega)}{[1 + \exp(-\hbar\omega/(kT))]} \equiv$$
$$[1 + \tanh(-\hbar\omega/(2kT))]J(w) \tag{9}$$

The semiclassical form of the spectral density is back Fourier transformed to yield a modified form of $M(t)$. The even

TABLE 4: Nonstandard MD Parameters and Charges for NADH
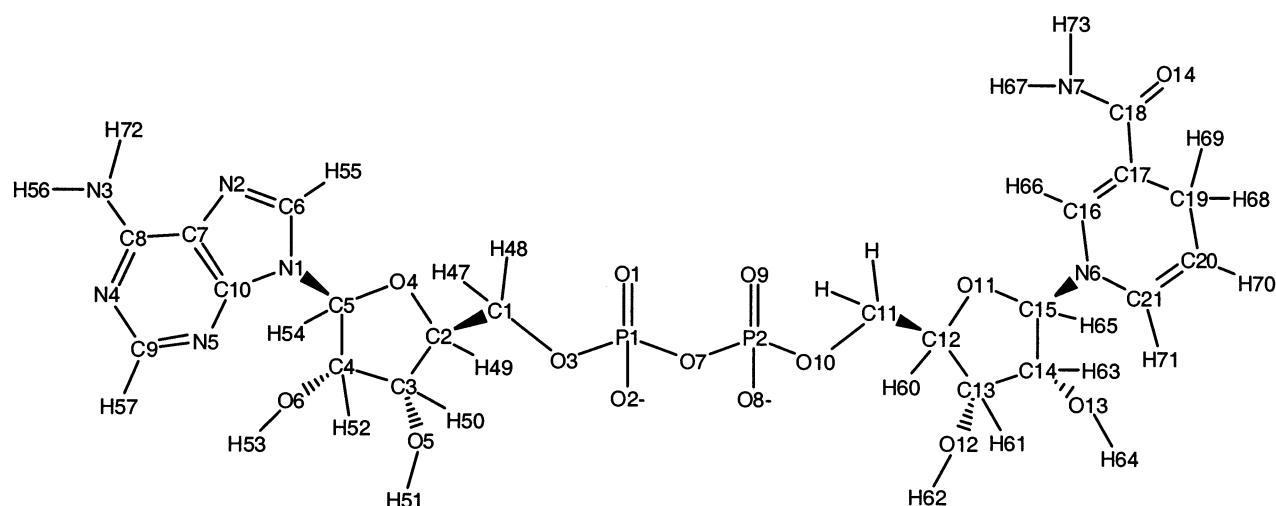
NADH Charges Common to All Three MD Simulations

atom	charge	atom	charge	atom	charge	atom	charge	atom	charge	atom	charge	atom	charge
P1	+0.942 262	C5	+0.148 989	C10	+0.287 632	O12	−0.688 179	C19	+0.003 584	H54	+0.120 526	H64	+0.393 708
O1	−0.751 784	N1	+0.003 740	O7	−0.389 268	C14	+0.085 110	C20	−0.257 754	H55	+0.182 914	H65	+0.163 577
O2	−0.751 784	C6	+0.074 646	P2	+1.085 819	O13	−0.624 314	C21	−0.066 683	H56	+0.374 708	H66	+0.116 496
O3	−0.393 707	N2	+0.594 769	O8	−0.772 815	C15	+0.037 068	H47	+0.082 207	H57	+0.073 409	H67	+0.374 674
C1	+0.018 558	C7	+0.164 769	O9	−0.772 815	N6	+0.011 980	H48	+0.082 207	H58	+0.101 734	H68	+0.035 385
C2	+0.064 412	C8	+0.558 570	O10	−0.430 385	C16	−0.109 296	H49	+0.110 945	H59	+0.101 734	H69	+0.035 385
O4	−0.408 559	N3	−0.777 933	C11	+0.027 083	C17	−0.106 001	H50	+0.074 971	H60	+0.074 556	H70	+0.162 816
C3	+0.291 031	N4	−0.740 753	C12	+0.060 268	C18	+0.651 558	H51	+0.399 284	H61	+0.062 116	H71	+0.162 816
O5	−0.656 568	C9	+0.512 274	O11	−0.391 394	O14	−0.617 698	H52	+0.013 375	H62	+0.443 688	H72	+0.374 708
C4	+0.173 011	N5	−0.683 413	C13	+0.249 868	N7	−0.864 974	H53	+0.390 589	H63	+0.160 887	H73	+0.374 674
O6	−0.605 416												

NADH Atom Types Common to All Three MD Simulations

atom	type	atom	type	atom	type	atom	type	atom	type	atom	type	atom	type
P1	P	O5	OH	C8	CA	O8	O2	C14	CT	H52	H1	H60	H1
O1	O2	C4	CT	N3	N2	O9	O2	O13	OH	H53	HO	H61	H1
O2	O2	O6	OH	N4	NC	O10	OS	C15	CT	H54	H2	H62	HO
O3	OS	C5	CT	C9	CQ	C11	CT	H47	H1	H55	H5	H63	H1
C1	CT	N1	N*	N5	NC	C12	CT	H48	H1	H56	H	H64	HO
C2	CT	C6	CK	C10	CB	O11	OS	H49	H1	H57	H5	H65	H2
O4	OS	N2	NB	O7	OS	C13	CT	H50	H1	H58	H1	H72	H
C3	CT	C7	CB	P2	P	O12	OH	H51	HO	H59	H1		

NADH Atom Types Specific to MD Simulations 2 and 3

atom	type	atom	type	atom	type	atom	type	atom	type	atom	type
N6	N*	C16	CM	C19	CT	H66	H4	H69	HC	H71	H4
N7	NZ	C17	CM	C20	CM	H67	HZ	H70	HA	H73	HZ
O14	OZ	C18	CZ	C21	CM	H68	HC				

Missing NADH Bond Parameters for MD Simulations 2 and 3

bond type	K_r (kcal/mol)	r_{eq} (Å)	bond type	K_r (kcal/mol)	r_{eq} (Å)
CZ-OZ	570.0	1.229	CZ-NZ	490.0	1.335
CM-CZ	410.0	1.444	NZ-HZ	434.0	1.010

Missing NADH Angle Parameters for MD Simulations 2 and 3

angle type	K_θ (kcal/mol)	θ_{eq}	angle type	K_θ (kcal/mol)	θ_{eq}	angle type	K_θ (kcal/mol)	θ_{eq}	angle type	K_θ (kcal/mol)	θ_{eq}
CT-CM-HA	35.0	118.0	CM-CZ-OZ	80.0	125.3	CM-CZ-NZ	70.0	117.3	CZ-NZ-HZ	30.0	120.0
CM-CT-CM	63.0	110.2	CT-CM-CZ	70.0	119.7	OZ-CZ-NZ	80.0	122.9	HZ-NZ-HZ	35.0	120.0
CM-N*-CM	70.0	117.8	CM-CM-CZ	63.0	120.7						

Missing NADH Dihedral Parameters for MD Simulations 2 and 3

dihedral	K_ϕ (kcal/mol)	ϕ	n	dihedral	K_ϕ (kcal/mol)	ϕ	n	dihedral	K_ϕ (kcal/mol)	ϕ	n
NZ-CZ-CM-CT	0.50[a]	180.0	2	OZ-CZ-CM-CT	0.40[a]	0.00	6	CM-CM-CZ-OZ	1.95[a]	180.0	2
NZ-CZ-CM-CT	0.35[a]	180.0	3	CM-CZ-NZ-HZ	2.50[a]	180.0	2	CZ-CM-CM-H4	0.10	180.0	2
NZ-CZ-CM-CT	0.40[a]	0.00	6	CM-CM-CZ-NZ	1.10[a]	180.0	1	CZ-CM-CM-N*	2.50	180.0	2
OZ-CZ-NZ-HZ	2.50[a]	180.0	2	CM-CM-CZ-NZ	1.95[a]	180.0	1	CZ-CM-CT-CM	1.00	180.0	3
OZ-CZ-CM-CT	1.00[a]	180.0	2	CM-CM-CZ-OZ	0.30[a]	180.0	1	CZ-CM-CT-HC	1.00	180.0	3
OZ-CZ-CM-CT	1.00[a]	0.00	3								

[a] These values were set to zero for simulation 3.

components of the function are determined by the real components in the Fourier domain, and the odd components are related to the complex components. With the transformation given by eq 9, the even part of the spectrum of oscillators—the real part of $M(t)$—is left unchanged, and only an odd component that delivers a complex part to $M(t)$ is added. This in turn imparts a complex component for the linear response function, resulting in a Stokes shift between the calculated absorption and emission spectra (eqs 7a and 7b).

Note that in the high-temperature limit, the above method yields the same result as the multimode Brownian oscillator (MBO) picture,[28] in which

$$g(t) = i\lambda \int_0^t M(\tau)\, d\tau + \Delta^2 \int_0^t d\tau_1 \int_0^{t_1} M(\tau_2)\, d\tau_2 \quad (10)$$

and in the high-temperature limit $\lambda = \hbar\Delta^2/(2kT)$, where λ is the reorganization energy, Δ is the root-mean-square energy gap fluctuation, k is Boltzmann's constant, and T is the temperature.

The time-varying transition dipole moment (TDM) (see eq 3) can also be included within the cumulant expansion approach for the calculation of the optical response. When constants in time are ignored, the linear optical response function becomes the product of three response functions derived from the energy gap and TDM autocorrelation functions and the cross correlation between the energy gap and TDM,[34] as shown in eq 11,

$$R(t) = \exp(-g_{dd}(t) + 2i\dot{g}_{\delta d}(t) + \ddot{g}_{\delta\delta}(t)) \quad (11)$$

where g_{dd} is the line broadening function already discussed and is derived from the energy gap autocorrelation function. The other line-broadening functions, $g_{\delta\delta}$ and $g_{\delta d}$, are derived in the same manner but substituting the energy gap autocorrelation function for the TDM autocorrelation function and the cross correlation between the energy gap and TDM, respectively. Detailed balance is asserted by adjusting the spectrum of oscillators for each individual correlation function using eq 9. We found that the inclusion of the time-varying TDM had a relatively small effect on the results.

References and Notes

(1) Mercer, I. P.; Gould, I. R.; Klug, D. R. *J. Phys. Chem. B* **1999**, *103*, 7720.

(2) Muino, P. L.; Callis, P. R. *J. Chem. Phys.* **1994**, *100*, 4093.

(3) Kumar, P. V.; Maroncelli, M. *J. Chem. Phys.* **1995**, *103*, 3038.

(4) Fleming, G. R.; Cho, M. H. *Annu. Rev. Phys. Chem.* **1996**, *47*, 109.

(5) Jimenez, R.; Fleming, G. R.; Kumar, P. V.; Maroncelli, M. *Nature* **1994**, *369*, 471.

(6) Mercer, I. P.; Gould, I. R.; Klug, D. R. *Faraday Discuss.* **1997**, 51.

(7) Amer, H. QM/MM Studies of Myoglobin. Ph.D. Thesis, Imperial College of Science, Technology and Medicine, London, 2001.

(8) Amer, H.; Walker, R. C.; Mercer, I. P.; Klug, D. R.; Gould, I. R., manuscript in preparation.

(9) Case, D. A.; Pearlman, D. A.; Caldwell, J. W.; Cheatham, T. E., III; Ross, W. S.; Simmerling, C. L.; Darden, T. A.; Merz, K. M.; Stanton, R. V.; Cheng, A. L.; Vincent, J. J.; Crowley, M.; Tsui, V.; Radmer, R. J.; Duan, Y.; Pitera, J.; Massova, I.; Seibel, G. L.; Singh, U. C.; Weiner, P. K.; Kollman, P. A. *AMBER 6*; University of California: San Francisco, CA, 1999.

(10) Brändén, C.-I.; Jörnvall, H.; Eklund, H.; Furugren, B. *The Enzymes*, 3rd ed.; Academic Press: New York, 1975; Vol. 11.

(11) Ramaswamy, S.; Scholze, M.; Plapp, B. V. *Biochemistry* **1997**, *36*, 3522.

(12) Shearer, G.; Kim, K.; Lee, K.; Wang, C.; Plapp, B. *Biochemistry* **1993**, *32*, 11186.

(13) Schafmeister, C. E. A. F.; Ross, W. S.; Romanovski, V. *Leap*; University of San Francisco: San Francisco, CA, 1995.

(14) Ryde, U. *Proteins: Struct., Funct., Genet.* **1995**, *21*, 40.

(15) Ryde, U. *Eur. Biophys. J. Biophys. Lett.* **1996**, *24*, 213.

(16) Ryde, U. *J. Comput.-Aided Mol. Des.* **1996**, *10*, 153.

(17) Cornell, W. D.; Cieplak, P.; Bayly, C. I.; Gould, I. R.; Merz, K. M.; Ferguson, D. M.; Spellmeyer, D. C.; Fox, T.; Caldwell, J. W.; Kollman, P. A. *J. Am. Chem. Soc.* **1995**, *117*, 5179.

(18) Pavelites, J. J.; Gao, J. L.; Bash, P. A.; Mackerell, A. D. *J. Comput. Chem.* **1997**, *18*, 221.

(19) Roothan, C. C. J. *Rev. Mod. Phys.* **1951**, *23*, 69.

(20) Binkley, J. S.; Pople, J. A.; Herhe, W. J. *J. Am. Chem. Soc.* **1980**, *102*, 939.

(21) Frisch, M. J.; Trucks, G. W.; Schlegel, H. B.; Scuseria, G. E.; Robb, M. A.; Cheeseman, J. R.; Zakrzewski, V. G.; Montgomery, J. A., Jr.; Stratmann, R. E.; Burant, J. C.; Dapprich, S.; Millam, J. M.; Daniels, A. D.; Kudin, K. N.; Strain, M. C.; Farkas, O.; Tomasi, J.; Barone, V.; Cossi, M.; Cammi, R.; Mennucci, B.; Pomelli, C.; Adamo, C.; Clifford, S.; Ochterski, J.; Petersson, G. A.; Ayala, P. Y.; Cui, Q.; Morokuma, K.; Malick, D. K.; Rabuck, A. D.; Raghavachari, K.; Foresman, J. B.; Cioslowski, J.; Ortiz, J. V.; Stefanov, B. B.; Liu, G.; Liashenko, A.; Piskorz, P.; Komaromi, I.; Gomperts, R.; Martin, R. L.; Fox, D. J.; Keith, T.; Al-Laham, M. A.; Peng, C. Y.; Nanayakkara, A.; Gonzalez, C.; Challacombe, M.; Gill, P. M. W.; Johnson, B. G.; Chen, W.; Wong, M. W.; Andres, J. L.; Head-Gordon, M.; Replogle, E. S.; Pople, J. A. *Gaussian 98*, revision A.7; Gaussian, Inc.: Pittsburgh, PA, 1998.

(22) Jorgensen, W. L.; Chandreskhar, J.; Madura, J. D.; Impey, R. W.; Klein, M. L. *J. Chem. Phys.* **1983**, *79*, 926.

(23) Bayly, C. I.; Cieplak, P.; Cornell, W. D.; Kollman, P. A. *J. Phys. Chem.* **1993**, *97*, 10269.

(24) Berendsen, H. J.; Postma, J. P. M.; Van Gunsteren, W. F.; DiNola, A.; Haak, J. R. *J. Chem. Phys.* **1984**, *81*, 3684.

(25) Essmann, U.; Perera, L.; Berkowitz, M. L.; Darden, T.; Lee, H.; Pedersen, L. G. *J. Chem. Phys.* **1995**, *103*, 8577.

(26) Foresman, J. B.; Head-Gordon, M.; Pople, J. A.; Frisch, M. J. *J. Phys. Chem.* **1992**, *96*, 135.

(27) Chandler, D.; Bader, J. S.; Kuharski, R. A.; Sprik, M.; Klein, M. L.; Impey, R. W. *J. Chem. Phys.* **1988**, *89*, 3248.

(28) Mukamel, S. *Principles of Nonlinear Optical Spectroscopy*; Oxford University Press: New York, 1995.

(29) Kubo, R. *J. Phys. Soc. Jpn.* **1962**, *17*, 1100.

(30) Kubo, R. *Adv. Chem. Phys.* **1969**, *15*, 101.

(31) Chandler, D. *Introduction to Modern Statistical Mechanics*; Oxford University Press: New York, 1987.

(32) Kubo, R. *Rep. Prog. Phys.* **1996**, *29*, 255.

(33) Mukamel, S. *J. Phys. Chem.* **1985**, *89*, 1077.

(34) Khidekel, V.; Chernyak, V.; Mukamel, S. *J. Chem. Phys.* **1996**, *105*, 8543.